

# BENCHMARKING OF DIFFERENT POWDER-BED METAL FUSION PROCESSES FOR MACHINE SELECTION IN ADDITIVE MANUFACTURING

E. Yasa\*, F. Demir\*, G. Akbulut\*, N.Cızıoğlu\*, S. Pilatin\*

\* TUSAS Engine Industries, Inc.

Eskişehir, Turkey

REVIEWED

## Abstract

In the last decade, additive manufacturing has gained significant interest for direct part production and started to change the way companies manufacture products; even in very demanding sectors like aerospace. The biggest challenge for a wider industrial acceptance still stands as the need for more reliable, repeatable and precise machines for additive manufacturing. This paper presents a comprehensive benchmarking study for the selection of an additive manufacturing machine for powder-bed metal fusion process, i.e. Selective Laser Melting or Direct Metal Laser Sintering or Laser Cusing. Four different machine vendors for the same technology to be employed for aeroengine part manufacturing using Inconel 625 powder have been involved for comparing different machine specifications. Many aspects such as dimensional accuracy, surface quality, need of support structures, density, hardness and process limits (minimum wall thickness, overhang surfaces, inclinations and curvatures, etc.) are addressed in the paper. The state-of-the-art in machines for powder-bed metal fusion process is presented aiming at understanding the current limitations of the technology available today.

## Introduction

Laser Beam Melting (LBM), also referred to as direct metal laser sintering/melting (DMLS/DMLM), Laser Cusing®, Selective Laser Melting® (SLM), is a powder-based, additive manufacturing process where a 3D part is produced, layer by layer, by using a high-energy lasers to selectively melt powdered materials which then fuse during solidification as defined in VDI 3404 (see Figure 1 for schematic LBM process). The process involves physical binding activated by the heating of the powder particles using the laser energy. Common post-processes to improve surface quality may include microblasting, laser re-melting or laser assisted material removal [1].

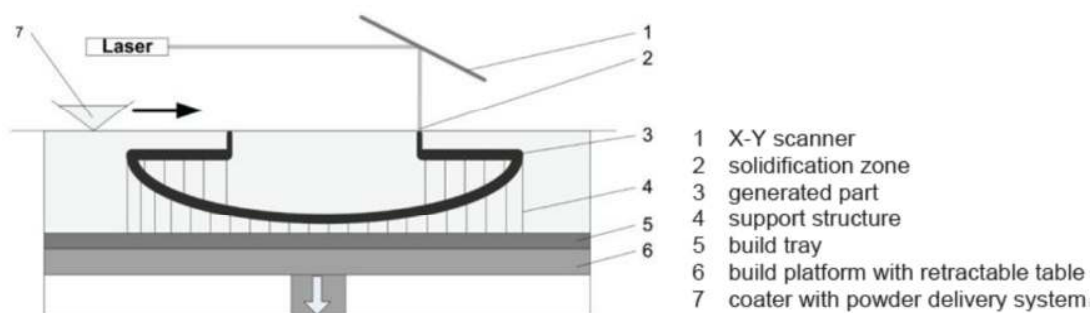


Figure 1: Schematical Laser Beam Melting process [1]

Among many additive manufacturing (AM) technologies, the processes suitable and commercially available for functional metallic materials using electron or laser as the energy source are demonstrated in Table 1. There are other technologies targeting metals such as sheet lamination or binder jetting but these are less relevant in terms of direct functional part production, but rather prototyping [2]. Depending on many criteria such as material suitability, surface roughness, accuracy, component size, needed post-processing technologies, etc. one has to decide which AM technology is best for her/his application. Choosing the needed AM technology is most of the times is not the final decision to be made (see Table 1). Among many machine vendors, the most suitable brand and model has to be decided, which is not always an easy process to accomplish. In case of laser beam melting, all machine vendors claim to manufacture the state-of-the-art machines and there is unfortunately no standard yet established for machine qualification or acceptance testing in the open literature. Companies in need of an LBM machine usually specify their own acceptance testing procedures or use the machine vendors' own established qualification procedures. Not only companies to buy a machine, but also the research institutes carry out benchmarking studies to compare different processes and also different machines. Some examples of benchmark designs are given in Figure 2. Various studies focus on determining the process capability in terms of different aspects. For example, Vandenbroucke and Kruth focused on identification of the process limits regarding the accuracy, surface roughness, density, mechanical properties and stair effect for two different materials, i.e. Ti64 and CoCr, for dental applications and the tests were carried out on one LBM machine, namely Concept Laser M3 machine. This study more aims at optimization of the process parameters for maximum part performance [8]. Kruth et al., in [9], compare different additive manufacturing technologies, i.e. Selective Laser Sintering -SLS and LBM, for evaluating these processes as rapid manufacturing technologies rather than rapid prototyping. As a result of this study, they have concluded that the real breakthrough of SLS and LBM technologies in other industries than medical parts and tooling inserts, depend on further improvements in process accuracy and productivity [9]. Campanelli et al., in [10], also investigates the process capabilities and performance of the LBM process by testing density, accuracy and mechanical properties. In this study, it is concluded that the process is capable of producing almost full density parts with good mechanical properties with a good accuracy for nominal dimensions greater than 400  $\mu\text{m}$ . For nominal dimensions lower than this value, the errors increase [10]. Although most of the studies target at exploring process capability/limits, some studies more focus on equipment comparison for a single process. Mantel, compares laser cusing, direct metal laser sintering and selective laser melting which are commercial names for the same process, i.e. LBM, respectively by Concept Laser, EOS and SLM Solutions [11]. Despite the fact that different materials were used for comparison for the same geometrical and material properties, different benchmark geometries were tested in this study concluding that Laser Cusing is the most promising LBM technology for different industrial sectors such as tooling, medical, aerospace and motor industry (see Figure 3 for comparison results for aerospace). However, taking the materials used in the study into account, that may be a misleading information. In this paper, the results of a benchmarking study carried out to select the most suitable LBM equipment for aerospace applications are presented. The procedure was first to design a benchmarking part, which is actually a modified version of the one presented in [3] due to timing issues (see Figure 4 for the design used in this study). This benchmark part design was sent to four LBM machine vendors (Renishaw, Concept Laser GmbH, EOS GmbH Electro Optical Systems, and SLM Solutions GmbH) to build the parts in Inconel 625. It was mainly specified that 1) Support structures may be utilized for overhang surfaces but they should be removed before shipment; 2) Heat treatments

only for stress relief may be applied on the parts; 3) Material removal processes such as grinding, polishing, benching are not allowed on any parts. After the parts were delivered by TEI, they were evaluated in terms of detail resolution, geometrical accuracy, surface quality, density and hardness comparing the results with each other.

Table 1: Various AM technologies and commercially available machine vendors for direct functional metallic parts using electron or laser as the energy source

	ELECTRON	LASER
POWDER	<p>ELECTRON BEAM MELTING</p> <p>ARCAM</p>	<p>Powder-bed based LASER BEAM MELTING</p> <p>Concept Laser, EOS, SLM Solutions, Realizer, Renishaw, 3D Systems</p> <p>Laser blown powder LASER CLADDING</p> <p>Huffman, OPTOMECH, Trumpf, Insstek, BeAM</p>
WIRE	<p>ELECTRON BEAM DIRECT MANUFACTURING,</p> <p>SCIAMY</p>	

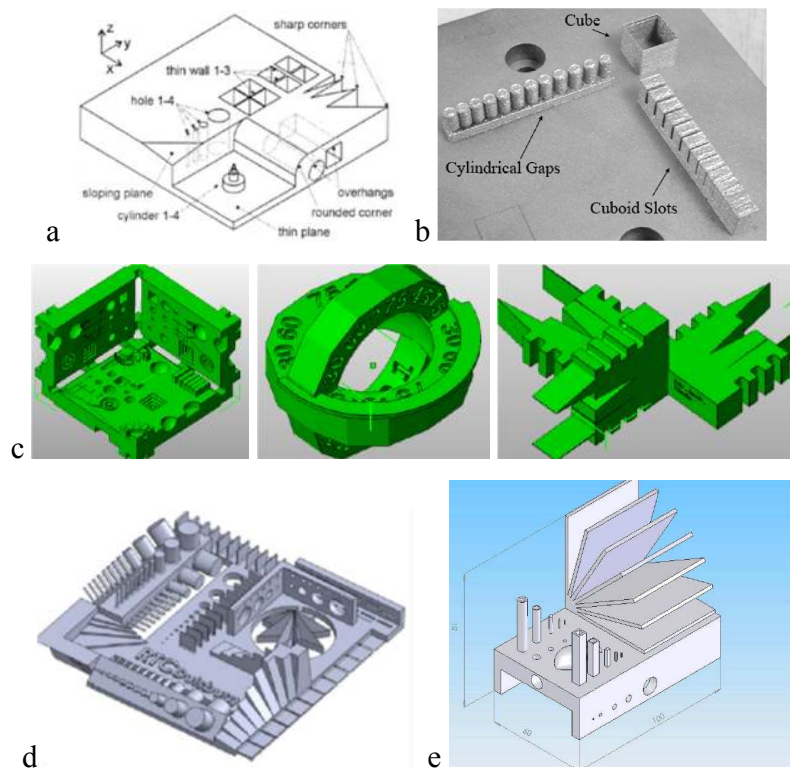


Figure 2: Benchmark designs from different studies a) [3] b) [4] c) [5] d) [6] e) [7]

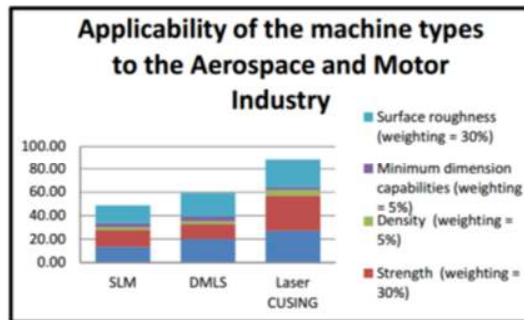


Figure 3: Benchmark test results regarding the aerospace and motor industry in [11]

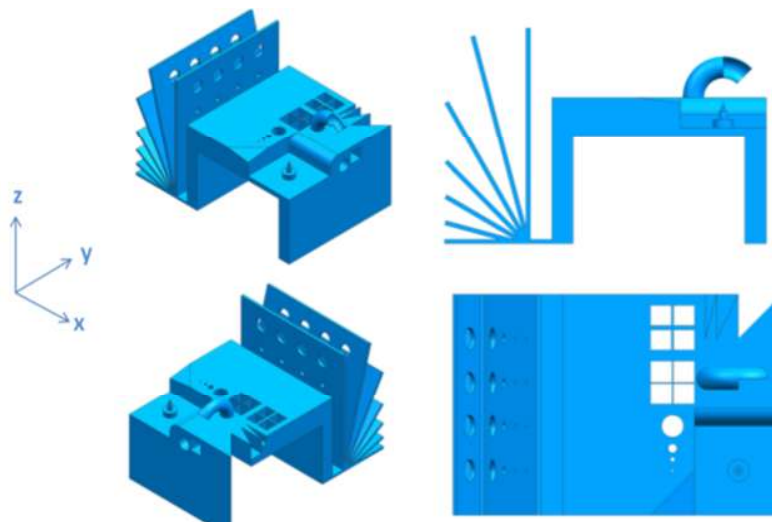


Figure 4: Benchmark design used in this study

### **Benchmark Geometrical Evaluation**

As a starting point, the part design were sent to all four machine vendors in .stp format and no specific direction for the build direction was given although in ASTM 52921 standard specifies z-axis as the build direction in its definition. Z-axis, for processes employing planar layerwise addition of material, shall run normal to the layers [12] (see Figure 5). The received benchmark parts from four machine vendors are shown with related build directions in Figure 6. As shown in the figure, not all machine vendors used the same axis for the build direction. For manufacturing the inclined walls with holes on, two of the machine vendors (V1 and V4) chose to build the benchmark part along Y-axis. In this case, there was no need to support the inclined walls whereas the small pin and the pipe detail needed to be supported. Although no polishing was allowed on the parts, probably due to very bad surface quality on the curved surface, some polishing may have been applied for the case of V4 as depicted in Figure 7a whereas Figure 7b shows the difficulty of making the boss detail in the selected build direction. The machine vendors were also asked to send the parts without supports which was not the case for V3. Moreover, during cutting the part from the base plate, the thin section connection overhang inclined walls and the main body was lost for V3. The geometrical details of the benchmark parts are demonstrated in Figure 8 regarding sharpness of vertical walls, boss, top surface, overhang

inclined walls, pipe detail and others. The geometrical details of the benchmark were generally made successfully by all four vendors with a few exceptions despite the quality difference. The summary of the results in terms of geometrical features are as follows:

- The sharp edges with different angles were best manufactured by V1 and V3 although they used a different build direction (all build directions were shown on the pictures. If not, it is from the page upwards or downwards). There is a lack of straightness for the sharp edges of V2 and V4 as shown in the first two rows of Figure 8.
- The boss detail is actually a tower of cylinders with decreasing radii as shown in the third row of Figure 8 (nominally from bottom to up 5, 2, 1 and 0.5 mm respectively). The smallest cylinder with a diameter of 0.5 mm was only successfully made by V3 with an accuracy of approximately 20  $\mu\text{m}$ . All others failed to produce the smallest diameter properly. The complete boss of V4 is unacceptable due to bad surface on the overhang side due to the build direction selection. The cylindricity of the boss made by V1 is also unacceptable due to the same reason. The surface quality and thus sharpness of the boss is best by V2 (see row 3&4 in Figure 8).
- The pipe detail is probably one of the most difficult features on the benchmark. The details of this feature on V3 is not clear due to supports. The selected build direction for V4 made it very difficult to produce this feature whereas V1 successfully made this feature along the same build direction with V4, probably due to good design of the supports. V2 has made it successfully with the cross formation on the overhang surface with a good surface quality both inside and outside of the feature (see row 5 in Figure 8).

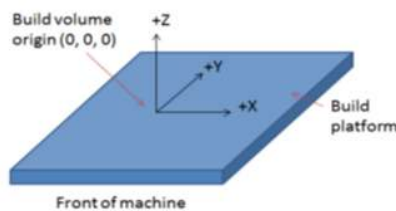


Figure 5: Generic AM machine system and coordinates [12]

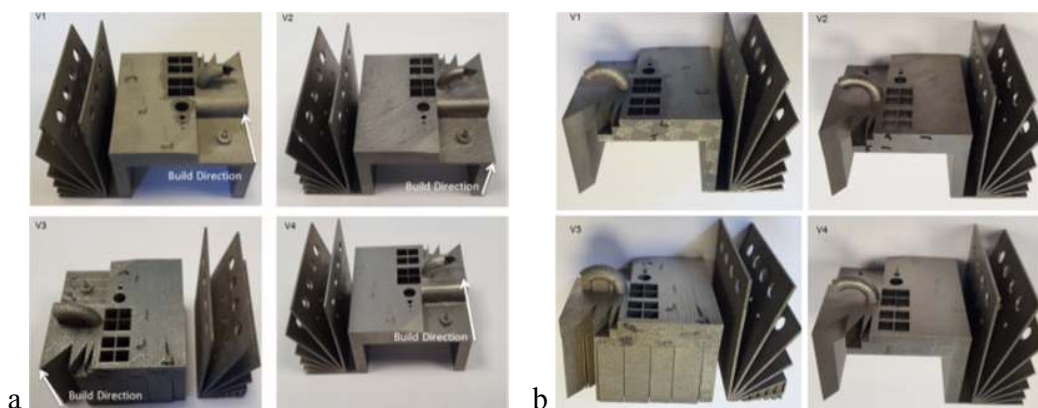


Figure 6: Benchmark parts from 4 different machine vendors with the utilized build directions<sup>1</sup> a) top view b) side view

<sup>1</sup> Machine vendors' names are on purpose not specified

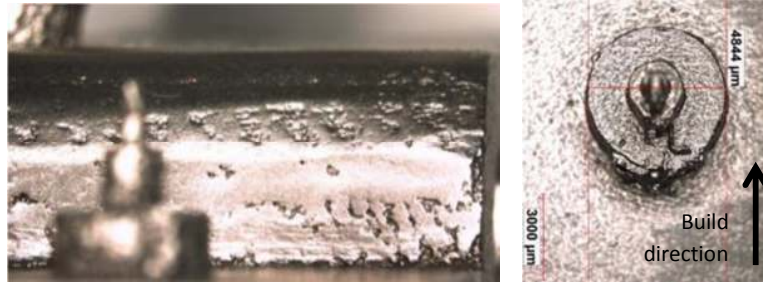


Figure 7: a) Traces of polishing b) overhang surfaces for the boss detail for V4

- The overhang inclined walls were successfully made by V1 and V4 due to the build direction. For V2 and V3, there was a need to support overhang walls with two maximum overhang angles. The removal of all support structures was successful for V2 (see Figure 9) although some particles remained trapped in the root (see row 6 in Figure 8).
- The holes with different diameters (5, 2, 1 and 0.5 mm) were best made by V2 with an accuracy of approximately 100  $\mu\text{m}$  whereas for V4 the accuracy for the hole diameters is around 200  $\mu\text{m}$ . Due to the selected build direction, V1 and V4 benchmarks show a dross formation on one side of the holes for almost all of the diameters. Moreover, the holes with a diameter of 1 and 0.5 mm are partially blocked for V1. For V3, the hole with a diameter of 0.5 is totally blocked whereas the hole with a diameter of 1 mm is partially blocked due to partially melted powder particles sticking in the holes (see row 7 in Figure 8).
- The overhang surface on the side of the benchmark all seem to be made with supports for the rectangular hole (see row 8 in Figure 8). However, the form of both features were not good for V1, V2 and V4 with accuracy values greater than 200  $\mu\text{m}$ . For V3, the geometrical accuracy was less than 100  $\mu\text{m}$  despite the support structure is still present for the rectangular geometry and makes it difficult to evaluate.
- The last observed feature is the thin walls with a nominal thickness of 250  $\mu\text{m}$ . For V4, it was not possible to make the walls in the build direction properly. For V1, the same problem appeared but the horizontal thin wall was manufactured with a higher thickness ( $\sim 580$   $\mu\text{m}$ ) due to dross formation whereas the straightness of the vertical wall is not acceptable. The best thin walls were made with V2 and V3. However, the side surface quality of the thin walls was very bad for V3 while the accuracy is higher than the one of V2 (see Figure 10 for details and dimensions).

### **Surface Roughness Evaluation**

In the scope of this study, only  $R_a$  and  $R_z$ , are taken into account for comparing four benchmark parts on two surfaces perpendicular to each other. As commonly known, average roughness,  $R_a$ , is the arithmetic mean of all deviations from the center line over the sampling path whereas  $R_z$  is the average distance between the five highest peaks and the five deepest valleys within the sampling length. The surface roughness in terms of average roughness ( $R_a$ ) and surface roughness depth ( $R_z$ ) are demonstrated in Figure 11 for four benchmark part with 95% confidence intervals. The surface roughness results were taken on two surfaces of the benchmark part as shown in Figure 12. As shown, taking the build directions differently, the top and side

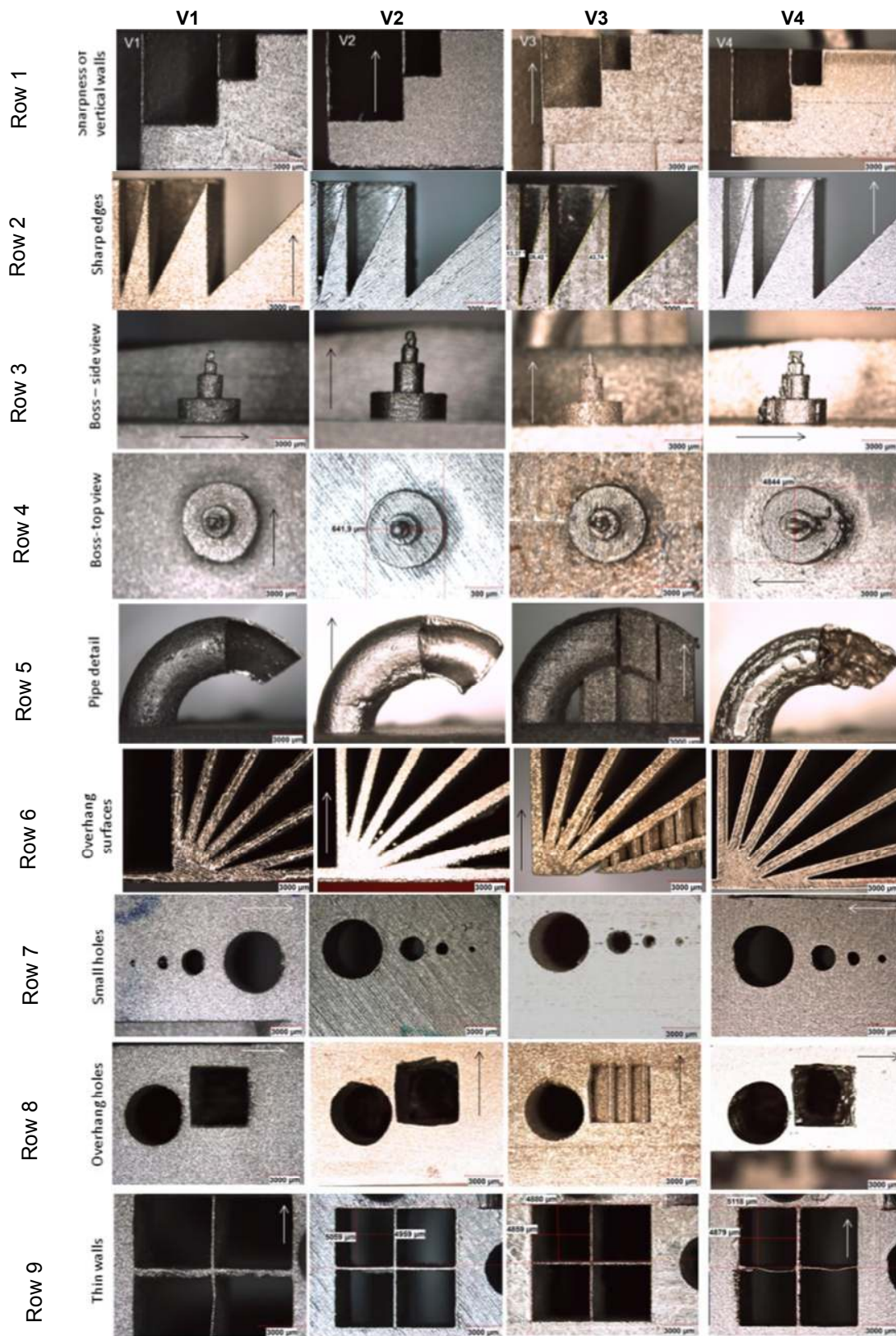


Figure 8 Benchmark details

surface definitions differ for V1 and V4. The measurements were taken with MarSurf M300 with a cutoff length of 2.5 mm, 3 repetitions and a sampling length of 12.5 mm. As Figure 11 depicts, the highest surface roughness ( $R_a$  and  $R_z$ ) on the side surface is exhibited by V3 whereas the highest surface roughness ( $R_a$  and  $R_z$ ) on the top surface is shown by V1. The trends in  $R_a$  and  $R_z$  are the same. V2 shows the lowest side surface roughness:  $R_a$  of  $3.9 \pm 1.4 \mu\text{m}$  and  $R_z$  of  $24 \pm 1 \mu\text{m}$  whereas V3 shows the lowest top surface roughness values:  $R_a$  of  $7 \pm 0.5 \mu\text{m}$  and  $R_z$  of  $35 \pm 3 \mu\text{m}$ . However, V3 shows 4 times higher roughness ( $R_a$ ) on the side surfaces compared to V2. Taking side and top surfaces into account, V2 and V4 gives the best and similar surface quality results.

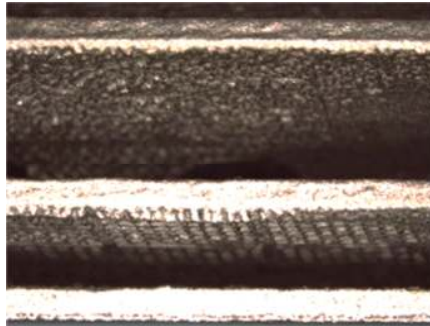


Figure 9: Remains from the support structures in the overhang inclined surfaces - V2

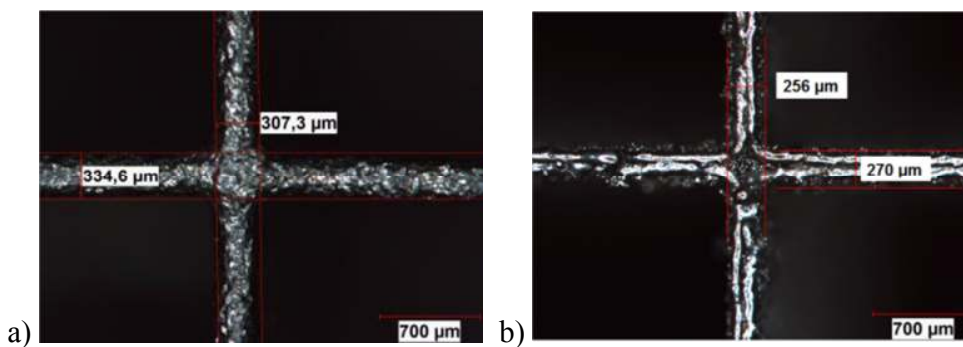


Figure 10: Thin wall details of a) V2 and b) V3

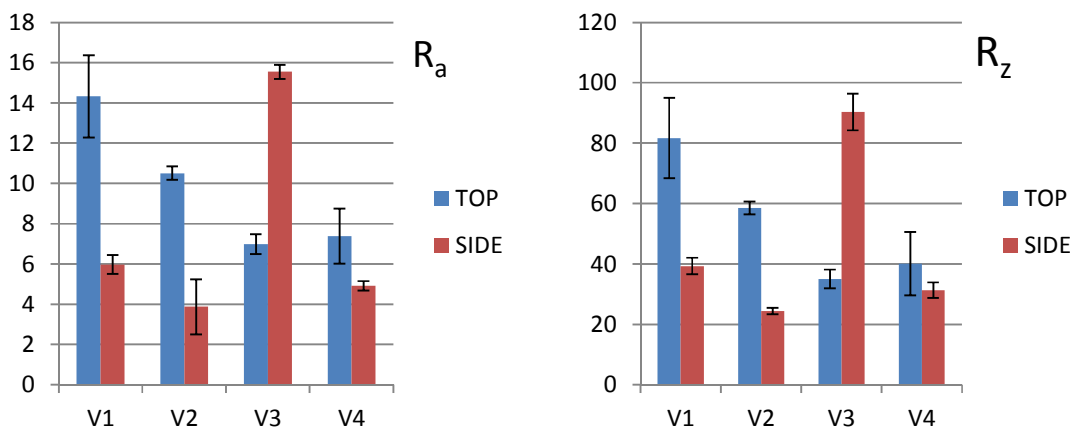


Figure 11: Surface roughness measurements a) Average roughness  $R_a$   
b) Surface roughness depth  $R_z$

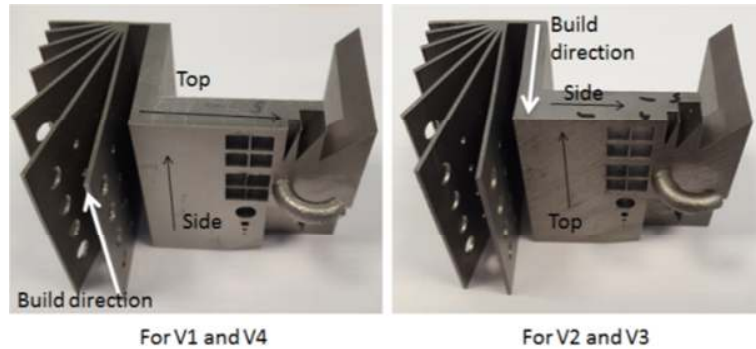


Figure 12: The surface roughness measurement directions for side and top surface notations

### Density Evaluation

For the evaluation of the density, two complementary methods were utilized: Archimedes' method and image analysis. For the Archimedes' method, the solid section, as shown in Figure 13 with red color, is cut from the benchmark part and divided into three equal parts. The density of each part was measured by Archimedes' method and  $8,44 \text{ g/cm}^3$  was taken as the reference density to calculate relative density for each benchmark part section [13]. Figure 14a shows the obtained results with 95% confidence intervals. V2 and V4 show densities above 99% whereas V3 has a relative density higher than 98%. Yet, V1 stays hardly above 97%. The results obtained from Archimedes' method are more global than image processing and do not give a clue for reasoning low densities. Thus, the cross-sections of specimens from the same block were observed to investigate the reason of such low values. An in-house developed Matlab code was utilized to calculate the porosity in the cross-sections. 3 images for each benchmark part were used and the average porosity values are shown in the Figure 14b where porosity values stay below 0.3% for all benchmark parts. One of the used images for each benchmark part is depicted in Figure 15. The image for V1 shows a high density as opposed to the values obtained by Archimedes' method. Some other sections from V1 were also measured by both methods and the results were the same. The reason may be a significant change of the chemical composition being different than others resulting in a lower density than  $8,44 \text{ g/cm}^3$ . The material compositions have not yet been investigated to be sure about this probability up to now. It can be concluded that laser beam melting gives almost full density for V2 and V4 with no problems associated. For V3, the lower density may a consequence of need of process parameter tuning or bad powder coating (see Figure 16 for traces).

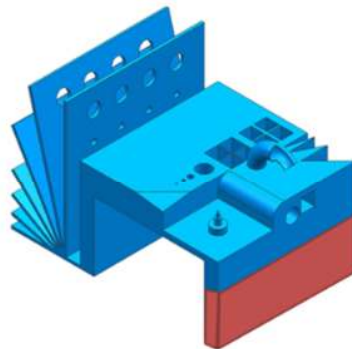


Figure 13: Section cut from the benchmark parts for density measurements

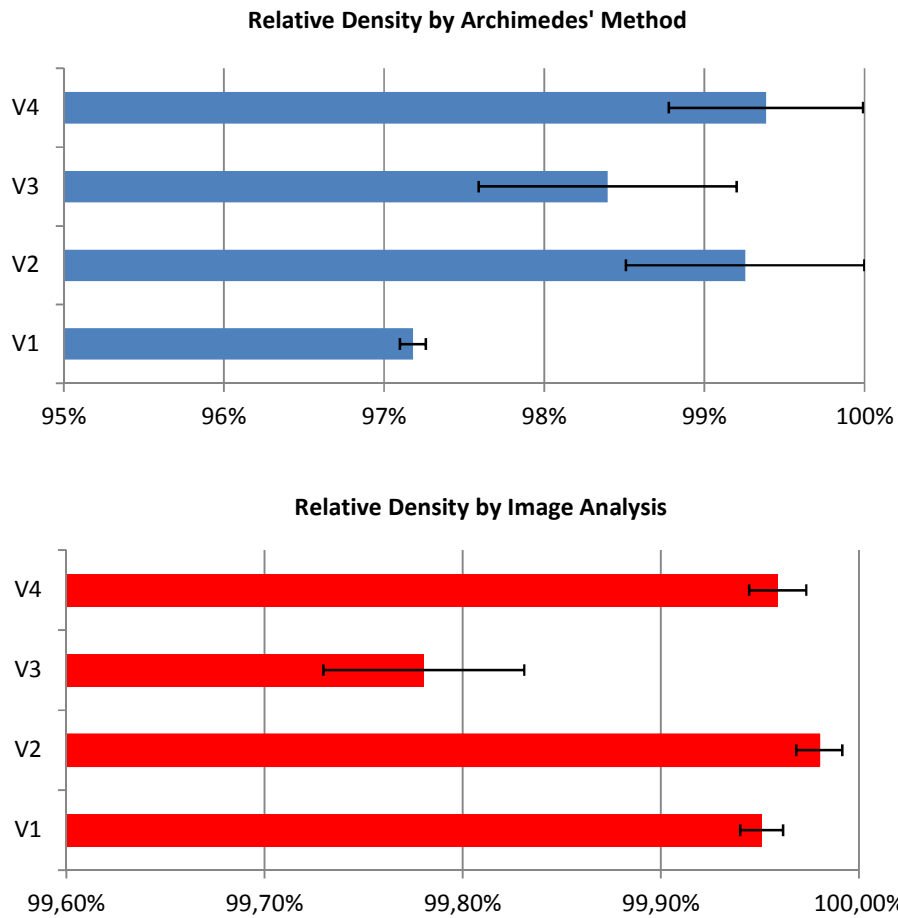


Figure 14: Relative density measurements by a) Archimedes' method  
b) Cross-sectional image analysis method

### Hardness Evaluation

Since hardness is a fast measure of many mechanical properties such as ductility, plasticity, strength and toughness, only hardness measurements were accomplished to get a quick and general idea of the mechanical properties obtained after LBM. Thus, microhardness of four benchmark parts were measured using indentation Vickers hardness using 500 gr force with approximately 10 s. The microhardness measurements were preferred against macrohardness measurements so that the results represent the material hardness but not the porosity. The measurements were taken using the same specimens used for density measurements on surfaces parallel to the build direction for all benchmark parts. 25 measurements were taken on each benchmark specimen. The results are demonstrated in Figure 17 with 95% confidence intervals. The highest hardness value is obtained from V2 with minimum deviation among different measurements ( $333 \pm 3$  HV) whereas the lowest hardness was derived from V4 with  $299 \pm 5$  HV. The values above 300 HV are in accordance to the values given by EOS Inconel 625 datasheet and other studies conducted with additive manufacturing of Inconel 625 [14-16]. Compared to the hardness obtained with solution strengthened Inconel 625 in wrought form and annealed

condition generally below 275 HV, laser beam melting leads to a higher hardness probably due to high cooling rates and fine microstructure [13].



Figure 15: Cross section samples used for density analysis

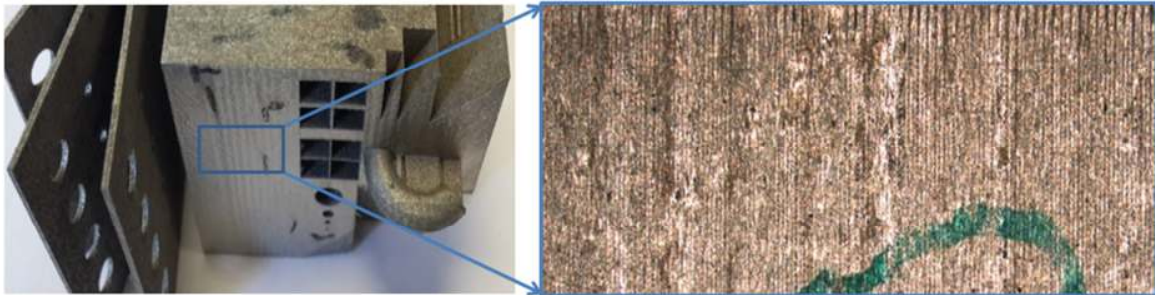


Figure 16: Waviness observed on the top surface of V3

The microstructures of the benchmark parts are also shown in Figure 18 and Figure 19 for different planes. Although a more detailed study is needed to evaluate the microstructures obtained, it can be stated that V1 shows a very fine and different microstructure compared to others. This also suggests a chemical composition variation as is suggested by density measurements. Figure 19 demonstrates a microstructure with fine dendrites and cells for both benchmark parts. Figure 19 also shows an apparent layering with curved melt scan bonding lines and the contrast provided to illustrate the melt bonds is probably due to  $\gamma''$  precipitates concentrating in these regions as also suggested by [17].

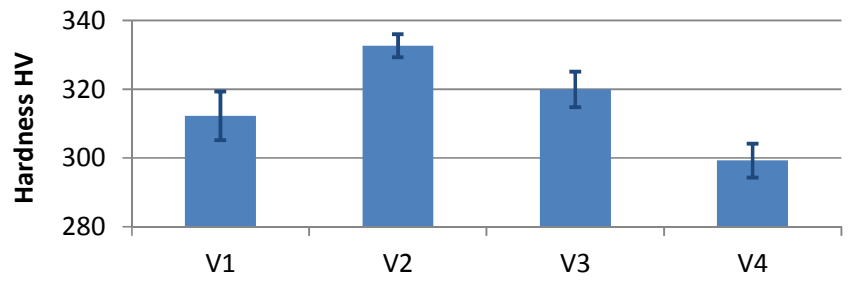
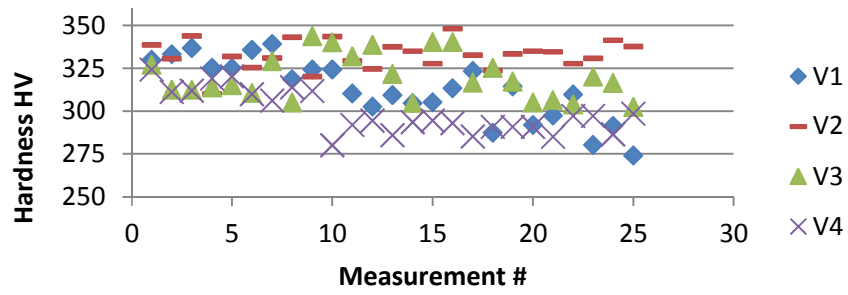


Figure 17: Microhardness test results

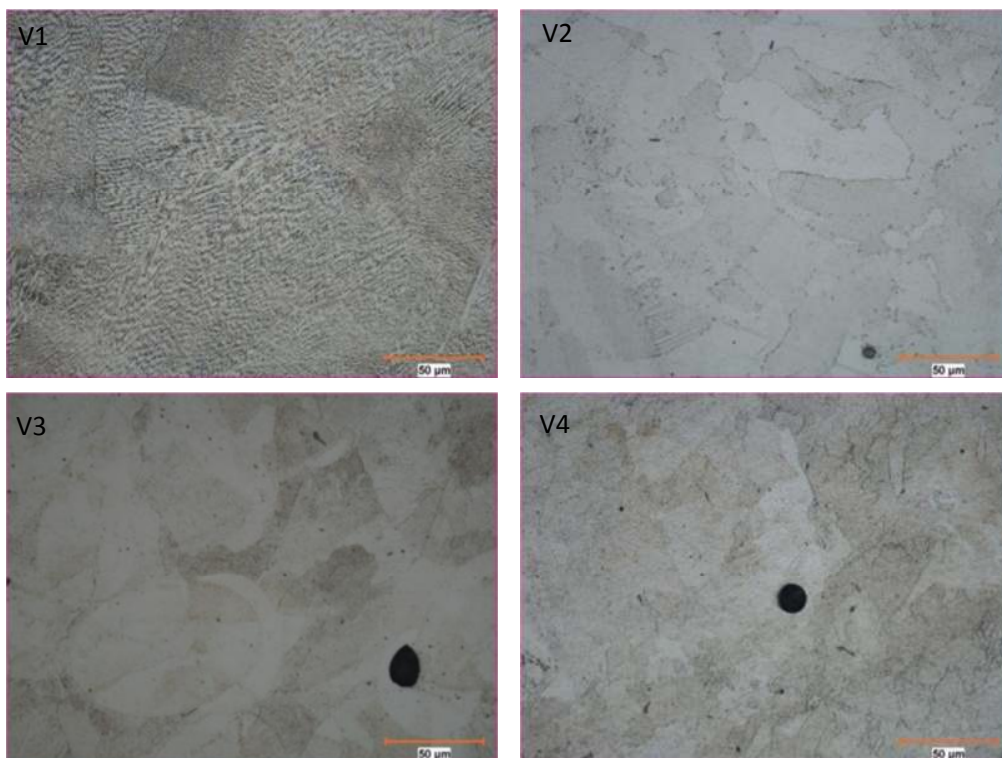


Figure 18: Microstructures in four benchmark parts (XY plane)

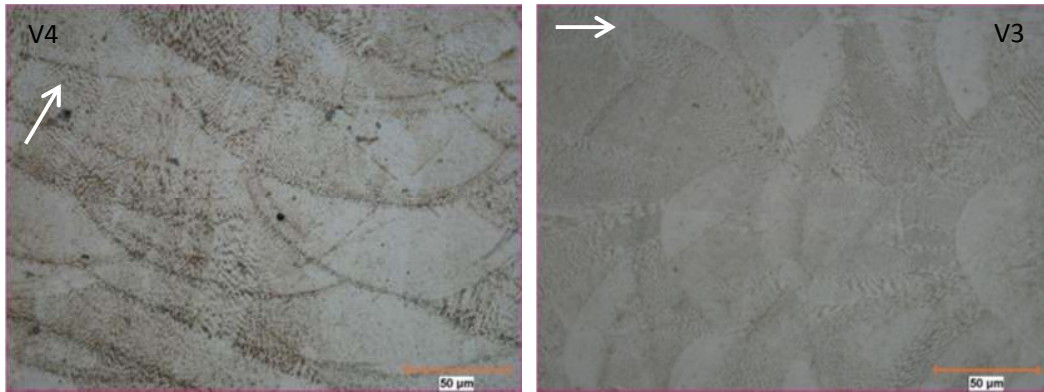


Figure 19: Apperant layering with curved melt scan bonding lines with the build directions shown for (XZ plane)

### **Conclusions**

A comprehensive benchmarking study for the selection of an additive manufacturing machine for laser beam melting process has been presented in this study. Four different equipment providers for LBM to be employed for aeroengine part manufacturing using Inconel 625 powder have been involved for comparing different machine specifications. Many aspects such as dimensional accuracy, surface quality, geometrical resolution, need of support structures, density, hardness and process limits are addressed in the paper. To conclude, it can be stated that laser beam melting technology is getting more and more mature every day for many diverse industrial sectors. However, it can still not be said that it is a directly plug and play technology for functional part production for applications with high requirements as commonly mistaken in public due to the easiness of personal 3D printers. For each application, in terms of part and material properties, the process has to be developed and optimized for best performance. Moreover, for the machine selectin, there are other factors than part properties, which should be taken into account such as equipment price, lead time, warranty time, consumables, optional functions or modules (data logging, powder coating or melt pool monitoring, processing in vacuum atmosphere, glass scale for linear drives, etc.) and so on. A decision matrix can be utilized to weigh each factor according to the specific needs.

### **Acknowledgements**

The authors would like to thank their colleagues at TEI; Özgür Poyraz, Rifat Yılmaz, Ezgi Uğur Solakoğlu, Soner Ören and Aydın Yağmur for the technical support and Undersecretariat for Defense Industries of Turkey in the scope of YAKUT project.

### **References**

1. VDI 3404 Additive Manufacturing Basics, definitions, processes, Draft version, Düsseldorf, May 2014.
2. Langefeld, B., 2013, Additive Manufacturing - A game changer for the manufacturing industry?, Roland Berger Strategy Consultants, Munich, November 2013.

3. Kruth, J.P., Vandenbroucke, B., Van Vaerenbergh, P., 2005, Benchmarking of different SLS/SLM processes as rapid manufacturing technologies, International Conference on Polymers and Moulds Innovations (PMI), p. 7, Gent, Belgium.
4. Thomas, D., 2009, Development of Design Rules for Selective Laser Melting, Ph.D. Thesis, University of Wales , Cardiff, UK.
5. Williams, C.B., Seepersad, C.C., 2012, Design For Additive Manufacturing Curriculum: A Problem- And Project-Based Approach, Technical Report, University of Texas at Austin, US.
6. Wegner, A., Witt, Gerd., 2012, Konstruktionsregeln für das Laser-Sintern, Zeitschrift Kunststofftechnik, Vol. 8, No. 3, pp. 253-277.
7. Castillo, L., 2006, Study about the rapid manufacturing of complex parts of stainless steel and titanium, Technical Report, TNO with the collaboration of AIMME.
8. Vandenbroucke, B., Kruth, J.-P., 2006, Selective Laser Melting of biocompatible metals for rapid manufacturing of medical parts, In Proc. Solid Freeform Fabrication, Austin, TX, USA.
9. Kruth, J.-P., Vandenbroucke, B., Van Vaerenbergh, J., Mercelis, P., 2005, Benchmarking of different SLS/SLM processes as rapid manufacturing techniques, Int. Conf. Polymers & Moulds Innovations (PMI), Gent, Belgium, April 20-23.
10. Campanelli, S.L., Contuzzi, N., Angelastro, A., Ludovico, A.D., 2010, Capabilities and Performances of the Selective Laser Melting Process, Chapter 13 in *New Trends in Technologies: Devices, Computer, Communication and Industrial Systems*, Edited by Meng Joo Er, ISBN 978-953-307-212-8, 454 pages, Publisher: Sciyo, Chapters published November 02.
11. Mantel, J.K., 2011, Capability Profile of an Additively Manufacturing Machine based on the Selective Laser Melting Process, Final Year Project in Department of Industrial Engineering, Stellenbosch University, South Africa.
12. ASTM 52921:2013 Standard terminology for additive manufacturing - Coordinate systems and test methodologies
13. [www.specialmetals.com/documents/Inconel%20alloy%20625.pdf](http://www.specialmetals.com/documents/Inconel%20alloy%20625.pdf) - Inconel® alloy 625 spec sheet
14. EOS material datasheet for Nickel Alloy IN625
15. Amato, K.N., Hernandez, J., Murr, L.E., Martinez, E., Gaytan, S.M., Shindo, P.W., Collins, S., 2012, Comparison of Microstructures and Properties for a Ni-Base Superalloy (Alloy 625) Fabricated by Electron and Laser Beam Melting, *Journal of Materials Science Research*, Vol. 1, No. 2; April 2012.
16. Kelbassa, I., Gasser, A., Meiners, W., Backes, G., Müller, B., 2012, High speed LAM, In Proc. of 37th MATADOR Conference, Manchester, UK, 25-27 July.
17. Murr, L.E., Martinez, E., Amato, K.N., Gaytan, S.M., Hernandez, J., Ramirez, A., Shindo, P.W., Medina, F., Wicker, R.B., 2012, Fabrication of Metal and Alloy Components by Additive Manufacturing: Examples of 3D Materials Science, *J. Mater. Res. Technol.* 2012;01:42-54 DOI: 10.1016/S2238-7854(12)70009-1.